Subdiffraction optical resolution of a gold nanosphere located within the nanojet of a Mie-resonant dielectric microsphere

Alexander Heifetz[1*], Jamesina J. Simpson[2], Soon-Cheol Kong[3], Allen Taflove[3], Vadim Backman[1]

[1]*Department of Biomedical Engineering, Northwestern University, Evanston, IL 60208*
[2]*Department of Electrical and Computer Engineering, University of New Mexico, Albuquerque, NM 87131*
[3]*Department of Electrical Engineering and Computer Sciencet, Northwestern University, Evanston, IL 60208*
*Corresponding author: a-heifetz@northwestern.edu

Abstract: We theoretically investigate light scattering from a bi-sphere system consisting of a gold nanosphere and a lossless dielectric microsphere illuminated at a resonant optical wavelength of the microsphere. Using generalized multisphere Mie theory, we find that a gold nanosphere 100 times smaller than the dielectric microsphere can be detected with a subdiffraction resolution as fine as one-third wavelength in the background medium when the microsphere is illuminated at a Mie resonance. Otherwise, off-resonance, the spatial resolution reverts to that of the nonresonant nanojet, approximately one-half wavelength in the background medium. An important potential biophotonics application is the detection of antibody-conjugated gold nanoparticles attached to the membranes of living cells in an aqueous environment.

©2007 Optical Society of America

OCIS codes: (290.1350) Backscattering; (290.5850) Scattering, particles; (290.4020) Mie theory; (170.3880) Medical and biological imaging.

References and links

1. C. Liang and Y.T. Lo, "Scattering by two spheres," Radio Sci **2**, 1481-1495 (1967).
2. R.T. Wang, J.M. Greenberg, D.W. Shuerman, "Experimental results of dependent light scattering by two spheres," Opt. Lett. **6**, 543-545 (1981).
3. G.W. Kattawar and C.E. Dean, "Electromagnetic scattering from two dielectric spheres: comparison between theory and experiment," Opt. Lett. **8**, 48-50 (1983).
4. M. I. Mishchenko and D. W. Mackowski, "Light scattering by randomly oriented bispheres," Opt. Lett. **19**, 1604-1606 (1994).
5. M. I. Mishchenko, L. D. Travis, and D. W. Mackowski, "Scattering of light by bispheres with touching and separated components," Appl. Opt. **34**, 4589-4599 (1995).
6. H. T. Miyazaki, H. Miyazaki, and K. Miyano, "Analysis of specular resonance in dielectric bispheres using rigorous and geometrical-optics theories," J. Opt. Soc. Am. A **20**, 1771-1784 (2003).
7. H.T. Miyazaki, H. Miyazaki, and K. Miyano, "Anomalous scattering by dielectric bispheres in the specular direction," Opt. Lett. **27**, 1208-1210 (2002).
8. S. P. Ashili, V. N. Astratov, and E. C. H. Sykes, "The effects of inter-cavity separation on optical coupling in dielectric bispheres," Opt. Express **14**, 9460-9466 (2006).
9. Z. Chen, A. Taflove, and V. Backman, "Photonic nanojet enhancement of backscattering of light by nanoparticles: A potential novel visible-light ultramicroscopy technique," Opt. Express **12**, 1214-1220 (2004).
10. X. Li, Z. Chen, A. Taflove, and V. Backman, "Optical analysis of nanoparticles via enhanced backscattering facilitated by 3D photonic nanojets," Opt. Express **13**, 526-533 (2005).
11. Z. Chen, X. Li, A. Taflove and V. Backman, "Super-enhanced backscattering of light by nanoparticles," Opt. Lett. **31**, 196-198 (2006).
12. A. Heifetz, K. Huang, A.V. Sahakian, X. Li, A. Taflove, V. Backman, "Experimental confirmation of backscattering enhancement induced by a photonic jet," Appl. Phys. Lett. **89**, 221118 (2006).
13. I. H. El-Sayed, X. Huang, and M.A. El-Sayed, "Surface plasmon resonance scattering and absorption of anti-EGFR antibody conjugated gold nanoparticles in cancer diagnostics: applications in oral cancer," Nano Lett. **5**, 829-834 (2005).

14. K. Sokolov, M. Follen, J. Aaron, I. Pavlova, A. Malpica, R. Lotan, and R. Richards-Kortum, "Real-time vital imaging of pre-cancer using anti-EGFR antibodies conjugated to gold nanoparticles," Cancer Res. **63**, 1999-2004 (2003).

15. Y.L. Xu, "Electronagnetic scattering by an aggregate of spheres," Appl. Opt. **34**, 4573-4588 (1995).

16. S. Tanev, V.V. Tuchin, P. Paddon, "Cell membrane and gold nanoparticles effects on optical immersion experiments with non-cancerous and cancerous cells: finite-difference time-domain modeling," J. Biomed. Opt. **11**, 064037 (2006).

17. A. Taflove and S. C. Hagness, *Computational Electrodynamics: The Finite-Difference Time-Domain Method*, 3rd ed. (Boston: Artech House 2005).

18. A. V. Itagi and W. A. Challener, "Optics of photonic nanojets," J. Opt. Soc. Am. A **22**, 2847-2858 (2005).

19. S. Lecler, Y. Takakura, and P. Meyrueis, "Properties of a three-dimensional photonic jet," Opt. Lett. **30**, 2641-2643 (2005).

20. S. Lecler, S. Haacke, N. Lecong, O. Crégut, J. -L. Rehspringer, and C. Hirlimann, "Photonic jet driven non-linear optics: example of two-photon fluorescence enhancement by dielectric microspheres," Opt. Express **15**, 4935-4942 (2007).

21. A. M. Kapitonov and V. N. Astratov, "Observation of nanojet-induced modes with small propagation losses in chains of coupled spherical cavities," Opt. Lett. **32**, 409-411 (2007).

22. Z. Chen, X. Li, A. Taflove, and V. Backman, "Enhanced backscattering of light by nanoparticles positioned in localized optical intensity peaks," Appl. Opt. **45**, 633-638 (2006).

23. H. C. van de Hulst, *Light Scattering by Small Particles* (Dover 1981).

24. P.W. Barber and R.K. Change (Editors), *Optical Effects Associated with Small Particles* (World Scientific 1988).

25. M.H. Fields, J. Popp, and R.K. Chang, "Nonlinear optics in microspheres," in *Progress in Optics* **41**, E. Wolf (editor), 1-96 (2000).

26. http://www.microspheres-nanospheres.com

27. P.B. Johnson and R.W. Christy, "Optical constants of the noble metals," Phys. Rev. B **6**, 4370-4379 (1972).

28. A. Giusto, S. Savasta, and R. Saija, "Nanoprobe control of morphology-dependent resonances of microspheres: A theoretical description," Phys. Rev. B **71**, 113415 (2005).

29. M. Sasaki, T. Kurosawa, and K. Hane, "Microobjective manipulated with optical tweezers," Appl. Phys. Lett. **70**, 785-787 (1997).

1. Introduction

Scattering by a bi-sphere system, which has potential applications to biomedical, atmospheric and ocean optics, has been investigated extensively over the last forty years, as for example [1-8]. In the past, the primary interest has involved scattering by a pair of spheres of similar size and composition.

Our group has recently been conducting theoretical, computational, and experimental investigations of optical scattering by microsphere/nanosphere bi-sphere systems wherein the sphere sizes differ by one to three orders of magnitude, and one of the spheres is a lossless dielectric while the other is metal [9-12]. One of the motivations for our research is to examine the feasibility of subdiffractional resolution of antibody-conjugated metal nanoparticles attached to the membranes of living cells in an aqueous environment. Antibody-conjugated noble metal nanoparticles have been shown to be useful in optical cancer detection [13,14]. Since the thickness of cellular membranes is approximately 10nm for most cells, i.e., essentially negligible, a reasonably good model is a bi-sphere system in an infinite water background medium, whether the metal nanoparticle is positioned on the exterior or interior surface of the membrane. Such a system can be analyzed with generalized multisphere Mie theory (GMM) [15]. A more comprehensive study that incorporates the effects of cellular membrane requires a more computationally involved FDTD study [16,17].

We have found that a plane-wave-illuminated lossless dielectric microsphere generates a photonic nanojet [9-12,18-21] propagating for a distance of approximately one wavelength in the background medium ($\lambda_{background}$) from the center of its shadow-side surface. The photonic nanojet is nonresonant, i.e., it exists over a wide range of the dielectric microsphere size parameter $x=2\pi a/\lambda_{background}$, where a is the radius of the microsphere. Furthermore, the full width at half maximum (FWHM) beamwidth of the nanojet is approximately at the diffraction limit, $\lambda_{background}/2$. Finally, the nanojet causes an effective giant enhancement of the

backscattering of a metal or dielectric nanoparticle located within the nanojet. That is, the backscattering of the dielectric microsphere is greatly perturbed by the presence of a nanoparticle within the nanojet such that a nanoparticle as small as $1/100^{th}$ of the size of the microsphere causes a perturbation comparable to the backscattering of the isolated microsphere [10-12]. In addition, we have shown that this perturbation follows a 3rd-power dependence on the nanoparticle diameter (for a fixed $\lambda_{background}$), unlike the Rayleigh scattering from an isolated nanoparticle which depends of the 6th power of the nanoparticle diameter [11,12]. In combination, these findings imply that nanoparticles as small as 5nm can be detected using visible light.

Although the backscattering perturbation caused by a nanoparticle located in a nonresonant photonic nanojet allows for its detection, the spatial resolution of this detection is limited by the transverse beamwidth of the nanojet, which is approximately $\lambda_{background}/2$. We have previously reported that FDTD simulations of plane-wave light scattering from a lossless dielectric spheroid reveal the presence of subdiffraction optical nanospots near the surface of the spheroid which are formed via near-field interference [22]. These nanospots extend a short distance outward from the spheroid's surface into the background medium. A nanoparticle positioned in one of these nanospots also causes a significant perturbation of the backscattering of the system. However, a spheroid generates a large number of approximately equal-amplitude nanospots distributed about its surface [22], and hence the location of the nanoparticle cannot be unambiguously determined.

2. Subdiffraction resolution

In this article, we investigate light scattering from a microsphere-nanosphere bi-sphere system, where the lossless dielectric microsphere is illuminated at a Mie-resonant wavelength [23]. We show via GMM solutions that, in this scenario, the location of the metal nanoparticle can be determined with subdiffraction $\lambda_{background}/2m$ resolution, where m is the refractive index contrast of the dielectric microsphere relative to its background medium. A key element for this improved detection resolution relative to that possible with a nonresonant nanojet is the formation of a morphology-dependent resonance (MDR), sometimes also referred to as a whispering gallery mode (WGM) [24,25]. These modes are standing waves formed just below the surface of a dielectric sphere or cylinder by counter-propagating waves undergoing total internal reflection. Briefly, MDR formation can be investigated by considering the backscattering cross-section of a dielectric microsphere, given by [24]

$$\sigma_b = \frac{\pi a^2}{x^2}\left|\sum_{n=1}^{\infty}(2n+1)(-1)^n(a_n - b_n)\right|^2 \qquad (1)$$

where x is the size parameter and a is the radius of a microsphere, and the expansion coefficients a_n and b_n are given by

$$a_n = \frac{j_n(x)[mxj_n(mx)]' - m^2 j_n(mx)[xj_n(x)]'}{h_n^{(2)}(x)[mxj_n(mx)]' - m^2 j_n(mx)[xh_n^{(2)}(x)]'} \qquad (2a)$$

and

$$a_n = \frac{j_n(x)[mxj_n(mx)]' - j_n(mx)[xj_n(x)]'}{h_n^{(2)}(x)[mxj_n(mx)]' - j_n(mx)[xh_n^{(2)}(x)]'} \qquad (2b)$$

where j_n is the spherical Bessel function of the first kind of order n and $h_n^{(2)}$ is the spherical Hankel function of the second kind of order n.

Mie resonances occur at the zeros of the denominators of a_n and b_n. The MDR's are characterized by the radial mode number l and the angular mode number n. For the sensing application reported in this article, we are interested in modes with $l=1$, which have longer evanescent decay distances compared to modes with larger l. Fig. 1 illustrates the shortest visible-wavelength (above 400nm in free space, 300nm in water) $l=1$ Mie resonance of a lossless 2μm diameter dielectric microsphere ($n_\mu = 2.0$) in water ($n_w = 1.33$). Here, the microsphere dielectric index contrast is $m=1.5$ relative to the water background. This microsphere is commercially available [26].
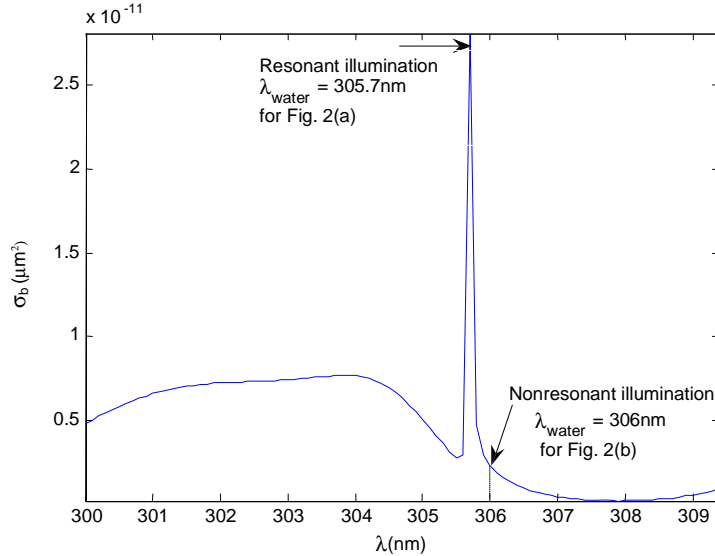
Fig. 1. Mie-series calculation of the backscattering cross-section σ_μ as a function of the wavelength λ_{water} for a lossless 2μm diameter dielectric sphere with the refractive index contrast $m=1.5$. The MDR mode of interest (1, 26) is at $\lambda_{water} = 305.7$nm.

Using near-field Mie theory, Fig. 2(a) visualizes the near-field intensity of the $l=1$, $n = 26$ MDR mode of the lossless 2μm diameter dielectric microsphere in water discussed above. The normalization is relative to the illumination, which is an x-polarized, z-propagating plane wave of $\lambda_{water} = 305.7$nm, exactly at the resonance shown in Fig 1. (The choice of $n = 26$ does not have a particular significance. The detection resolution is determined by the width of the fringe of the standing-wave pattern, which is equal to $\lambda/2m$, regardless of the angular mode number.) From Fig. 2(a), we observe that the null-to-null periodicity of the standing wave in the angular direction within the microsphere is $\lambda_{water}/2m$ (here, $\lambda_{water}/3$). This is equivalent to an FWHM intensity beamwidth of $\lambda_{water}/4m$ (here $\lambda_{water}/6$). We also see that the field in the fringe of the MDR mode evanescently leaks out from the microsphere into the background water medium. Due to diffraction, the FWHM beamwidth observed in the fringe zone increases. In the present example, the increase is from $\lambda_{water}/6$ to $0.3\lambda_{water}$ at a distance of 80nm from the back surface of the microsphere. Note that 80nm is less than the $1/e^2$ intensity decay length in the direction of propagation for this case, which is 130nm or $0.42\lambda_{water}$.

By way of comparison, Fig. 2(b) illustrates the normalized near-field intensity distribution for the microsphere of Fig. 2(a) at a slightly detuned illuminating wavelength of $\lambda_{water} = 306$nm (referring to Fig. 1). Here, we observe the generation of a nonresonant photonic nanojet having an FWHM intensity beamwidth of $0.5\lambda_{water}$ observed 80nm from the surface of the microsphere.

We next consider the resonant and nonresonant illumination cases of Figs 2a and 2b, respectively, with the addition of a 20nm diameter gold nanoparticle ($n_v = 1.47 - i1.95$ at the

incident frequency, m_v = 1.11-i1.47) [27] located at a variable distance from the back surface of the microsphere along its longitudinal axis. Using an available GMM code [15], we calculated the perturbation to the backscattering cross-section σ of the microsphere caused by the presence of the nanoparticle for each case. This perturbation is defined as

$$\Delta\sigma_{\mu+\nu} = \frac{\sigma_{\mu+\nu} - \sigma_\mu}{\sigma_\mu} \tag{3}$$

where $\sigma_{\mu+\nu}$ is the backscattering cross-section of the microsphere/nanosphere system, and σ_μ is the backscattering cross-section of the isolated microsphere. Results of these calculations are shown in Fig. 3.
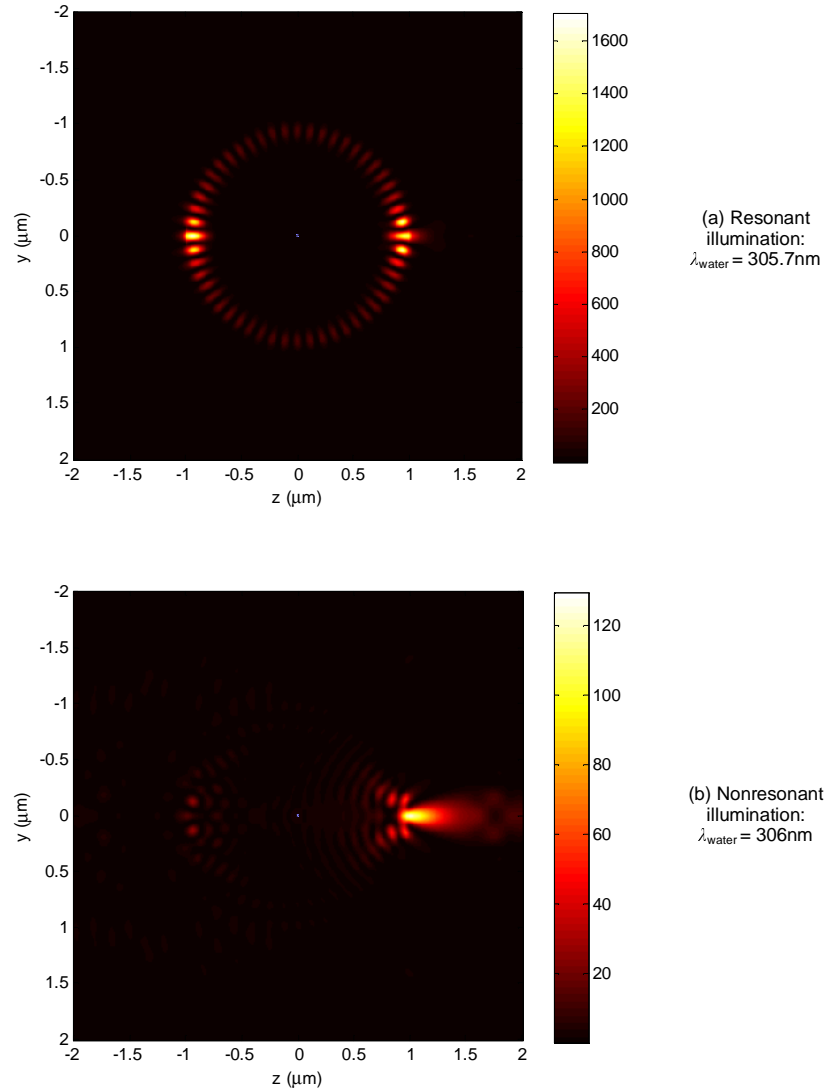
Fig. 2. (a) Visualization of the normalized optical intensity in the **H**-plane for resonant illumination. The MDR mode l=1 n=26 is obtained with near-field Mie code for a lossless 2μm diameter dielectric microsphere with index contrast m=1.5 at the resonant wavelength λ_{water} = 305.7nm. (b) Optical intensity visualization in the **H**-plane for nonresonant illumination at λ_{water} = 306nm.

From Fig. 3, we see that, for the case of nonresonant illumination, the backscattering cross-section from the microsphere/nanosphere system oscillates within the range −20% to +15% about the value of the backscattering from the isolated microsphere as the 20nm gold particle is moved from the back surface of the microsphere to a separation distance (to the center of the nanoparticle) of 500nm. This is because the nanoparticle retroreflects light from the nanojet that interferes either constructively or destructively with the light backscattered by the microsphere. For the case of resonant illumination, the composite backscattering cross-section oscillates within the range −13% to +3% about the value due to the isolated microsphere over the same 500nm separation range. However, when the separation is less than the decay length of the MDR fringe evanescent field, the composite backscattering cross-section is always lower than that due to the isolated microsphere. This is because at resonance, the backscattering perturbation is negative due to degradation of the MDR mode [28].
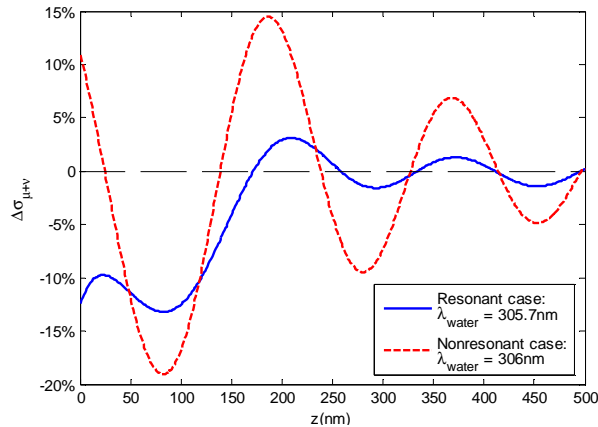

Fig. 3. GMM-calculated perturbation of the backscattering cross-section of the lossless 2μm-diameter dielectric microsphere caused by the variable positioning of a 20nm gold nanosphere from the back surface of the microsphere along the longitudinal axis. The microsphere is illuminated at the resonant wavelength λwater = 305.7nm (blue curve) and the nonresonant wavelength λwater = 306nm (red curve). Distance z is the location of the center of the nanosphere from the back surface of the microsphere.

Next, we consider the resonant and nonresonant illumination cases of Figs. 2a and 2b with regard to their capability to locate the 20nm gold particle in the transverse H−field direction at a fixed longitudinal separation of 80nm from the back surface of the microsphere. Fig. 4 illustrates computed GMM results for the backscattering perturbation $\Delta\sigma_{\mu+v}$ for the microsphere/nanosphere system for each case. From this figure, we see that the FWHM width of the dip of the backscattering cross-section for the resonant-illumination case is 100nm or $\lambda_{water}/3$, whereas the FWHM width for the nonresonant case is 160nm or $\lambda_{water}/2$.

Furthermore, we show that, using the resonant illumination wavelength λ_{water} = 305.7nm, it is possible to resolve the position of two 20nm-diameter gold nanospheres having a center-to-center separation of 100nm = $\lambda_{water}/3$ in the transverse H-direction. The nanospheres are located along a transverse line that is spaced 80nm from the back surface of the 2μm-diameter lossless dielectric microsphere. Fig. 5(a) shows the GMM-calculated backscattering perturbation of the three-sphere system $\Delta\sigma_{\mu+2v}$ as the pair of gold nanospheres is translated along the H-direction. For comparison, the backscattering perturbation $\Delta\sigma_{\mu+v}$ for a single gold nanosphere at λ_{water} = 305.7nm is plotted on the same graph. From Fig 5a, we see that the position of each nanosphere is evidenced by an approximate 3% fluctuation of the backscattering perturbation $\Delta\sigma_{\mu+2v}$. We expect that this fluctuation, approximately -15dB relative to the peak response, could be readily observed given the >50dB dynamic range of existing instrumentation.
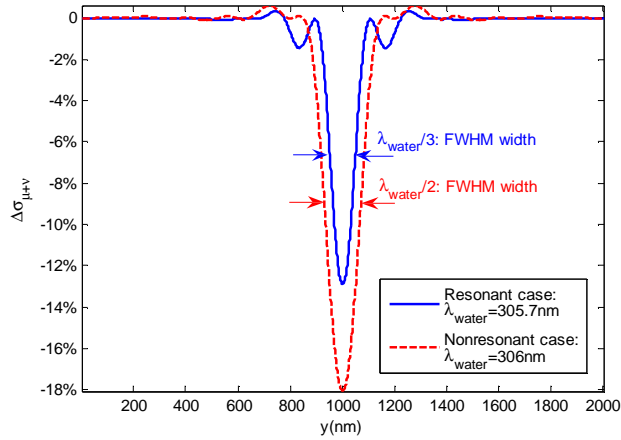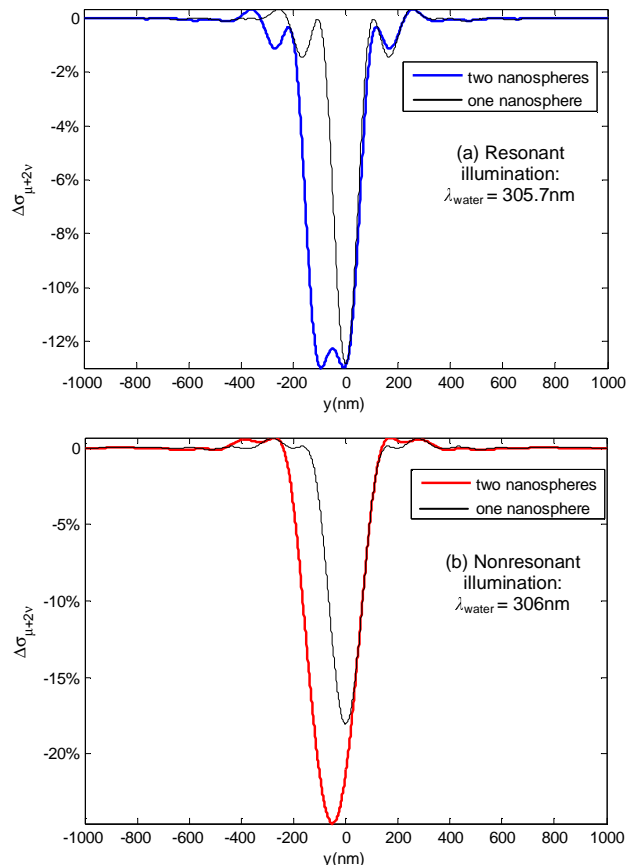
Fig. 4. GMM-calculated perturbation of the backscattering cross-section of the lossless 2μm-diameter dielectric microsphere as a function of the transverse position of the 20nm-diameter gold nanosphere relative to the longitudinal axis in the **H**-direction. The gold nanosphere is at a distance $z = 80$nm from the back surface of the dielectric microsphere.

Fig. 5. GMM-calculated perturbation of the backscattering cross-section of the lossless 2μm-diameter dielectric microsphere as a function of the transverse position of a pair of 20nm-diameter gold nanospheres having a fixed center-to-center separation of 100nm = $\lambda_{water}/3$. The nanospheres are located along a transverse line that is spaced 80nm from the back surface of the dielectric microsphere. The pair of gold nanospheres is translated transversely relative to the longitudinal axis in the **H**-direction. (a) $\lambda_{water} = 305.7$nm. (b) $\lambda_{water} = 306$nm.

Fig. 5(b) shows the results of the numerical experiment of Fig. 5(a) repeated at the nonresonant nanojet illumination wavelength λ_{water} = 306nm. As seen from this Fig., the position of each of the two golden nanospheres cannot be resolved.

Finally, we investigate the dependence of the MDR-facilitated backscattering perturbation $\Delta\sigma_{\mu+\nu}$ on the size of the nanosphere for a fixed wavelength. For the 2μm dielectric microsphere of Fig. 2(a) (resonant illumination λ_{water} = 305.7nm), we calculated the backscattering perturbations resulting from the presence of a gold nanoparticle having a variable diameter in the range of 14nm to 50nm located at a fixed distance of 80nm from the back surface of the microsphere to the center of the nanoparticle. Fig. 6 graphs the results of this study. We see that the absolute value of the backscattering perturbation almost exactly matches a cubic fitting polynomial, which is the lowest-order fitting polynomial. This indicates that, unlike the Rayleigh backscattering from an isolated nanoparticle which depends on the 6th power of the diameter of the nanoparticle for a fixed illuminating wavelength, the MDR-facilitated backscattering perturbation depends on the 3rd power of the nanoparticle diameter. This is the same behavior as for the nonresonant nanojet-induced backscattering perturbation, as reported earlier [11,12].
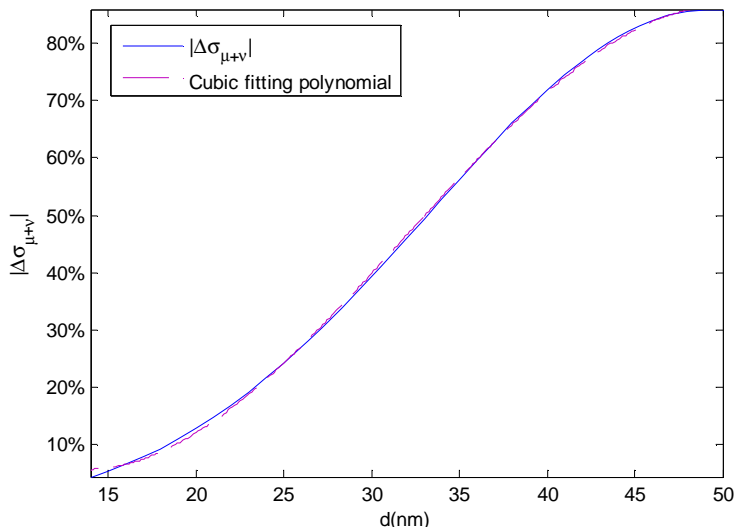

Fig. 6. GMM-calculated 3rd-power dependence of the absolute value of the backscattering cross-section perturbation $|\Delta\sigma_{\mu+\nu}|$ upon the nanosphere diameter d. Note that the illuminating wavelength is fixed at λ_{water} = 305.7nm, the (1, 26) MDR mode of the dielectric microsphere of Fig. 2(a). Rayleigh scattering from the isolated nanosphere would have a 6th-power dependence on d for a fixed wavelength.

3. Discussion and conclusions

As a possible application of the above findings, a scanning microsphere illuminated at a resonant wavelength can be used as a near-field surface microscopy tool having subdiffraction spatial resolution. The results of this study have shown the feasibility of a potential biophotonics application involving the detection of nanoparticles attached to the membranes of living cells in an aqueous environment. In a conceptual experiment, a cell could be scanned with an optically trapped microsphere [29], which would have a soft-spring recoil and hence would minimize damage to the biological sample. In such an experiment, the MDR mode of a lossless 2μm-diameter dielectric microsphere in water having a dielectric contrast of m = 1.5 could be excited at λ_{water} = 305.7nm with a tunable ring dye laser. (This corresponds to a laser output in air at 406.6nm, which falls within the ring dye laser's operational bandwidth of 370nm to 860nm with a 10MHz spectral linewidth.) Note that, as shown in Fig. 1, there are no

additional resonances within a spectral band of at least 3nm. Modes with such spectral separation can be resolved with a ring dye laser.

In summary, using the generalized multisphere Mie theory, we theoretically investigated optical plane-wave backscattering from a bi-sphere system in a water background medium. This system consisted of a lossless 2μm-diameter dielectric microsphere and a 20nm-diameter gold nanosphere illuminated at either a resonant ($l = 1$ whispering-gallery mode) or a nonresonant optical wavelength of the microsphere. We found that the nanosphere can be located with a subdiffraction transverse spatial resolution in the $\boldsymbol{H}-$direction as fine as $\lambda_{\text{water}}/3$ for the resonant case when the nanosphere is approximately $\lambda_{\text{water}}/4$ behind the microsphere. The backscattering perturbation signal that locates the nanosphere is no more than one order of magnitude below the backscattering of the isolated microsphere, even though the nanosphere is only $1/100^{\text{th}}$ the diameter of the microsphere. Furthermore, this perturbation signal diminishes only as the 3rd power of the nanosphere diameter. This is much slower than the Rayleigh 6th-power dependence for a fixed wavelength. All of these attributes lead to the possibility of using a conventional visible-light laboratory setup to detect and locate with subdiffraction resolution nanoparticles as small as a few nanometers.

Acknowledgments